Modeling for simulation of hybrid drivetrain components

Please check the document version of this publication:

Modeling for simulation of hybrid drivetrain components

T. Hofman, and M. Steinbuch
Technische Universiteit Eindhoven
Dept. of Mech. Engineering,
Control Systems Technology Group,
PO BOX 512, 5600 MB Eindhoven,
The Netherlands
Email: t.hofman@tue.nl

R.M. van Druten
Drivetrain Innovations B.V.
Horsten 1, 5612 AX Eindhoven,
The Netherlands
Email: druten@dtinnovations.nl

Abstract—Designing a hybrid drivetrain is a complex task, due to the unknown sensitivity of vehicle performance to system components specifications, the interaction between systems components, and the ability to operate the system components at different set points at any time. Therefore, many researchers [1-6] have made efforts formulating, and developing holistic hybrid drivetrain analysis, design, and optimization models including the top-level vehicle system control. However, an integral design approach [6] is usually characterized by large computation times, complex design problem formulations, multiple subsystem simulations, analyses, and non-smooth, or non-continuous models. In this paper, the influence of the component efficiencies, whereby the engine operation strategy (engine-, or system optimal operation) on the fuel economy, and the Energy Management Strategy (EMS) is investigated. Thereby, a relative simple Rule-Based (RB) EMS [11] is used, and is compared with the strategy based on Dynamic Programming (DP). The series-parallel transmission of the Toyota Prius has been used as a case study. The component modeling, and simulation results from the RB EMS, and DP are compared with results from the simulation platform ADVISOR. Finally, it is shown, that modeling the component efficiencies by only a few characteristic parameters, and using the RB EMS, the fuel consumption can be calculated very quickly, and with sufficient accuracy. In future work, the influence of topology choice on the fuel economy, and the EMS will also be investigated.

I. INTRODUCTION

In this paper component modeling for simulation will be investigated. Thereby, the main research question is: Is it possible with *sufficient* accuracy to describe the component efficiencies by a limited set of parameters using power-based functions? Thereby, it is defined, that it is sufficient if it is possible for a certain passenger car:

i To calculate the fuel consumption on a drive cycle with a certain accuracy;

ii To develop an Energy Management Strategy (EMS).

This will be demonstrated by using a series-parallel type of hybrid drivetrain, which will be analyzed, and validated by simulation.

A. Contribution, and outline of paper

The modeling, and simulation results will be compared with results from the simulation platform ADVISOR [2] for the Toyota Prius. The models in ADVISOR describing the EMS, and the characteristics of the hybrid drivetrains are developed based on test data, provided by the National Renewable Energy Laboratory (NREL), and Argonne National Laboratory (ANL) [9], [10]. The EMS plays an important role in an effective usage of the drivetrain components. A commonly used technique for determining the globally optimal EMS is DP [7], [8]. The contribution of this paper is that,

- DP will be used to determine the EMS, whereby the sub-optimal strategy as is implemented in ADVISOR is significantly improved;
- The influence of component efficiencies, whereby the engine operation strategy (engine -, or system optimal operation), on the fuel economy, and the EMS will be investigated.
- A new, and simple Rule-Based EMS will be used (as is discussed in [11]), and with using the characteristic parameters describing the component efficiencies it will be shown that the fuel economy, and EMS can be calculated very quickly, and with sufficient accuracy.

The hybrid drivetrain modeling, and simulation approach is discussed in Section II. Thereby, the power-based functions describing the component efficiencies are discussed. The control strategies in order to investigate the component efficiencies on the fuel economy is discussed in Section V. The engine -, Transmission (T), and Secondary power source (S) modeling are discussed in the Sections III, and IV respectively. The simulation results are discussed in Section VI. Finally, the conclusions, and outlook are discussed in Section VI-B.

II. SYSTEM MODELING, AND SIMULATION APPROACH

A classification overview of different example transmissions for hybrid drivetrain topologies is shown in the Fig. 1. In the Fig. 1 also the black box model describing S, and T is shown. For the series -, and the series-parallel transmission the advantage is that S (battery, power electronics, and electric machine) is integrated with T. For the parallel transmission S is connected at the engine-side of T. The variator of the series -, and the parallel transmission consists respectively of two electric machines, and a push-belt Continuously Variable

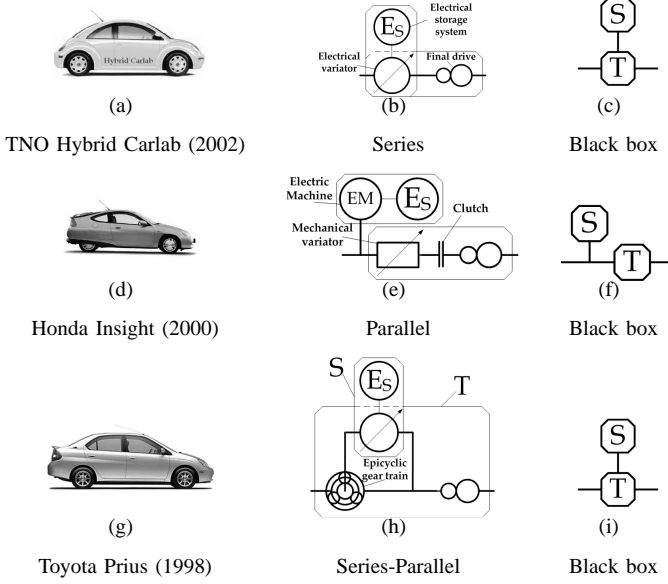Transmission (CVT). One of the major advantages of the

Fig. 1. Different hybrid technologies, and topologies.

series transmission is the Infinitely Variable Transmission (IVT) ratio. Thereby, it is possible to operate the engine, and the generator intermediate, but continuously at its highest efficiency point(s). However, at higher requested vehicle loads, the transmission losses of the electrical variator are typically larger than compared to a mechanical variator. The CVT losses in the parallel transmission are lower at higher vehicle loads, but usually due to the overdrive constraint not all optimal operating points of the engine can be reached reducing the overall vehicle performance. The series-parallel transmission combines the electrical -, and mechanical paths with its advantages, which consists of a planetary gear set combined with two electric machines, which form the variator part of T. The advantages of a series-parallel transmission, compared to a series transmission are:

- The transmission efficiency is higher, because most of the power is transmitted over the mechanical branch;
- An electrical variator with a lower maximum power throughput can be used.

However, a disadvantage is the possible occurrence of re-circulation of power flow thereby reducing the transmission efficiency. The operation of the variator, and the influence of the battery power on the power flows, and the overall efficiency will be discussed in more detail in Section III.

A. Simulation model, and power-based component modeling

The vehicle simulation model with the torque -, and the angular speed definitions are shown in Fig. 2. The fuel power P_f request to the engine is calculated backwards starting at the vehicle wheels. The power distribution between the different energy sources, i.e., fuel tank with stored energy E_f, S with stored energy E_s, and the vehicle driving over a drive cycle

represented by a required energy E_v. The efficiencies of the fuel combustion in the engine, or Primary power source (P), the storage and electric motor S, and the Transmission (T) are described by the variables η_P, η_S, and η_T respectively. The transmission speed ratio is represented by the variable r. In this paper static power-based models as discussed in
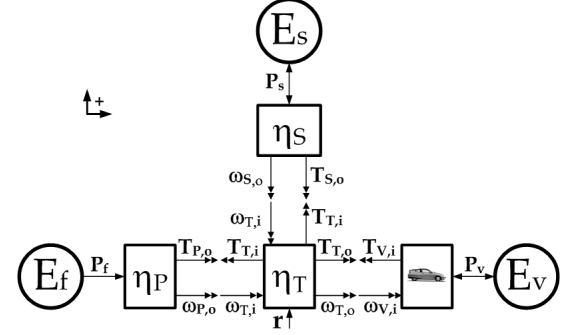

Fig. 2. Black-box free-body model for a hybrid drivetrain.

[12] describing the efficiency of the components are used. The advantages are, that it incorporates hardly any dynamics, and is therefore efficient in use. The only dynamic equation, which is an integrator, holds for the energy storage system. If an affine relationship is assumed, then the input power P_i as a function of the angular speed ω_o given the output power P_o becomes,

$$P_i = \phi(\omega_o|P_o) \approx c_1(\omega_o|P_o) \cdot P_o + c_0(\omega_o|P_o) \quad (1)$$

with the inverse efficiency ϕ, the fixed power losses c_0, and the reciprocal of the inner efficiency c_1. Both coefficients are dependent on operation point. The transmission technologies, power electronics, and electric machines are approximated by this first order function, while the battery, and the engine are approximated by a second order function in order to capture the high power-loss effects. Since, the static losses play an important role in the component efficiency, another advantage of this description is, that it is possible to determine these static losses quite well. In contrary to measuring -, or estimating the efficiency on-line, because for low powers approaching zero, the efficiency which is the ratio of the output -, and input power is difficult to determine.

III. ENGINE MODELING

The energy specific fuel consumption β is a function of $\omega_{P,o}$, and $T_{P,o}$ as is shown in Fig. 3(a) for the Toyota Prius (1998). If $P_{P,o}$ is specified $P_f = \phi_P(\omega_{P,o}|P_{P,o})$ becomes a function of $\omega_{P,o}$ alone, i.e.,

$$P_f = \beta\left(\omega_{P,o}, T_{P,o}\right) P_{P,o} h_{lv} = \beta\left(\omega_{P,o} \left| \frac{P_{P,o}}{\omega_{P,o}} \right.\right) P_{P,o} h_{lv} \quad (2)$$

The variable h_{lv} represents the lower heating value for fuel. The Engine Optimal Operation Line (EOOL) connects the optimal operation points, i.e., $\omega_{P,o}^*$, and $T_{P,o}^* = P_{P,o}/\omega_{P,o}^*$ fulfilling the condition of minimum fuel power,

$$\frac{\partial}{\partial \omega_{P,o}} \phi_P\left(\omega_{P,o}|P_{P,o}\right) = 0. \quad (3)$$

For the 1.5 l SI VVTi engine the EOOL almost coincides with the Wide-Open Throttle (WOT) torque line. In the Fig. 3(a) also the operation lines are shown for higher fuel consumptions in percentage of the values at the EOOL. The above equation is solved numerically, and in addition $\omega_{P,o}^*$ for each given $P_{P,o}$ gives solutions in the form of the function curve $P_f = \phi_P(\omega_{P,o}^*|P_{P,o})$ as is shown in the Fig. 3(b).
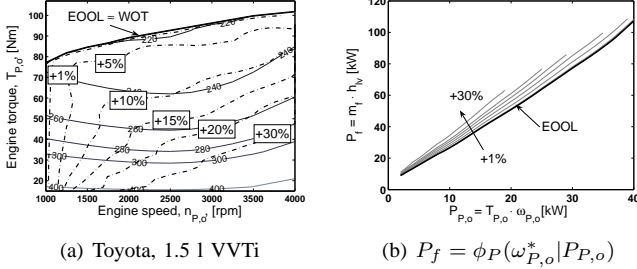
(a) Toyota, 1.5 l VVTi   (b) $P_f = \phi_P(\omega_{P,o}^*|P_{P,o})$

Fig. 3. Static-efficiency map in energy specific fuel consumption $[g/kWh]$ of the Toyota, 1.5 l VVTi (43 $[kW]$@4000 $[rpm]$), and the fuel input power as a function of the mechanical output power.

IV. TRANSMISSION, AND SECONDARY POWER SOURCE MODELING

A. Electric variator efficiency

In the Fig. 4(a), and (b), the static efficiency maps[1] of the generator $EM2$, and the motor $EM1$ including the inverter/controller efficiencies of the electric variator of the Prius (1998) are shown. In Fig. 4(d), all the input powers given the angular speeds as a function of the output powers of the electric machines are plotted. If a linear line is fitted through the data, the input power of $EM1$, and $EM2$ becomes,

$$P_1 = \phi_{em1}(\omega_{vo}|P_{vo}) \approx \phi_{em1}(P_{vo}) = \bar{c}_{11} \cdot P_{vo} + \bar{c}_{01}, \quad (4)$$

$$P_{vi} = \phi_{em2}(\omega_{vi}|P_2) \approx \phi_{em2}(P_2) = \bar{c}_{12} \cdot P_2 + \bar{c}_{02}. \quad (5)$$

given the battery output power $P_{bat} = 0$ (see also Fig. 4(c)). Accordingly, the variator efficiency η_v is,

$$\eta_v = \frac{P_{vo}}{P_{vi}} = \frac{1}{\bar{c}_{11}\bar{c}_{12}} - \left(\frac{1}{\bar{c}_{12}} + 1\right)\frac{\bar{c}_{02}}{\bar{c}_{11}}\frac{1}{P_{vi}}, \quad (6)$$

It can be seen with Eq. (6), that for

$$\lim_{P_{vi}\to\infty} \eta_v = \frac{1}{\bar{c}_{11}\bar{c}_{12}} = 0.77.$$

If $P_{bat} \neq 0$, then P_1 changes, and therefore also its efficiency. This is shown in the Fig. 5. In Fig. 5(a), P_2 is plotted as a function of T_{vi} for different fixed ω_{vi}. Note that P_2 as a function of T_{vi} given a certain ω_{vi} is well approximated by a linear, or quadratic function, while the contour efficiency map of Fig. 4(a) shows a strong non-linear dependency on torque, and speed. If the P_2 is increased by increasing the

[1]Note that only the first quadrant is measured by UQM Technologies. The power losses are mirrored to the other quadrants in order to calculate the efficiencies, which results in $\eta_{EM}(\omega_{EM}, -T_{EM2}) = 2 - 1/\eta_{EM}(\omega_{EM}, T_{EM2})$.

(a) 15 kW, AC PM syn. motor   (b) 30 kW, AC PM syn. motor

(c) Free-Body Model of electric variator with battery system   (d) $P_1 = \phi_{EM1}(P_{vo}|\omega_{vo})$, and $P_{vi} = \phi_{EM2}(P_2|\omega_{vi})$
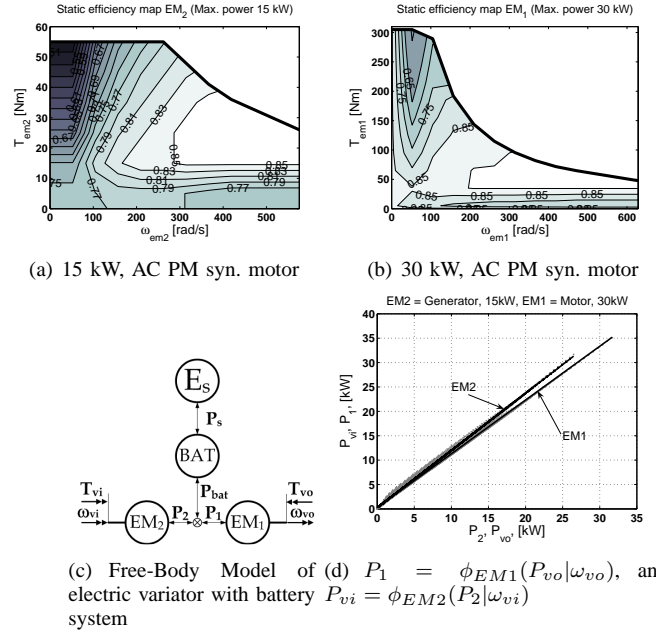
Fig. 4. Static efficiency maps of the electric machines of the Toyota Prius. The bold curves in (a), and (b) are the maximum torque as a function of speed.

TABLE I

AVERAGE FIT COEFFICIENTS

Power $[kW]$	EM_i	$\bar{c}_{1i}$ $[-]$	$\bar{c}_{0i}$ $[W]$	$\bar{e}_i$ $[W]^\dagger$
30	EM_1	1.10	297	3.9
15	EM_2	1.17	249	4.2

$\dagger$ average absolute error with a 99% confidence interval.

battery charging power for a certain output power, then T_{vi} has to be increased as well. If P_{vi} is calculated for different $P_{vo} \in \{0, 30\}$ $[kW]$, and $P_{bat} \in \{-30, 10\}$ $[kW]$, then it is possible to fit the following linear function through these data,

$$P_{vi} = \phi_v(P_{vo}|P_{bat}) \approx \bar{c}_1(P_{bat}) \cdot P_{vo} + \bar{c}_0(P_{bat}). \quad (7)$$

This is shown in Fig. 5(b). The dependency of the reciprocal of the average internal efficiency $\bar{c}_1$, and the static losses $\bar{c}_0$ as a function of P_{bat} are plotted in the figures 5(c), and (d) respectively. In Fig. 5(c) it can be seen that $\bar{c}_1$ is minimized around $P_{bat} \approx [-10, -5]$ $[kW]$.

B. Battery efficiency

The battery output power is the difference between P_s, and the battery losses $P_{s,loss}$ (see Fig. 4(c)),

$$P_{bat} = P_s - P_{s,loss} = V_{oc}(SoC, P_{bat}, \tau) \cdot I - I^2 \cdot R_i(SoC, \tau), \quad (8)$$

with the open circuit voltage V_{oc}, the current I, and the internal battery resistance R_i, both are dependent on State-of-Charge (SoC) of the battery. The battery operation temperature is represented by the variable τ. Since, the absolute internal storage capacity of the battery is very high, and the SoC fluctuation is within a narrow band, for simplicity, the battery efficiency η_{bat} has assumed to be independent on the SoC
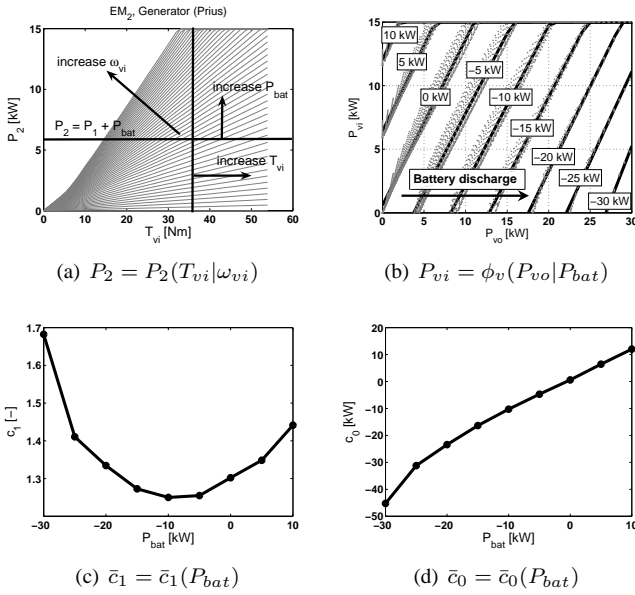
(a) $P_2 = P_2(T_{vi}|\omega_{vi})$

(b) $P_{vi} = \phi_v(P_{vo}|P_{bat})$

(c) $\bar{c}_1 = \bar{c}_1(P_{bat})$

(d) $\bar{c}_0 = \bar{c}_0(P_{bat})$

Fig. 5.   Influence of battery power on electric variator efficiency

(a) Internal resistance, R_i

(b) Open-circuit voltage, V_{oc}

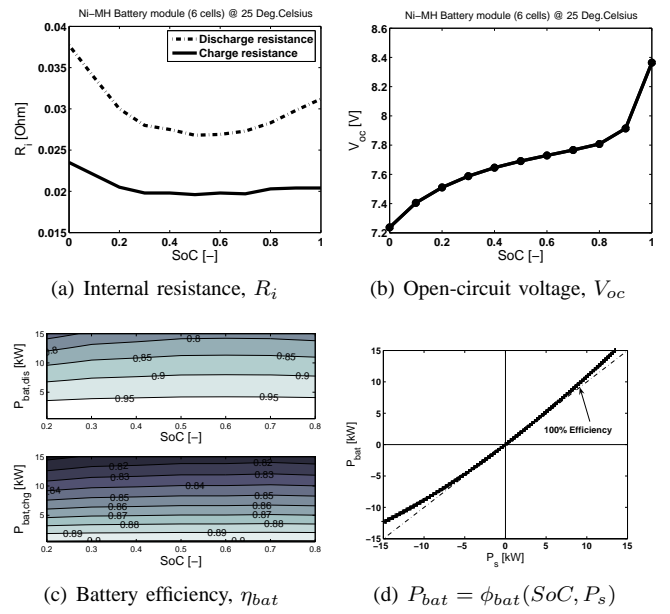(c) Battery efficiency, η_{bat}

(d) $P_{bat} = \phi_{bat}(SoC, P_s)$

Fig. 6.   Static efficiency maps for charging, and discharging of a Ni-MH Battery Pack consisting of 40 modules with $288V_{dc}$ bus voltage

level, and τ. Furthermore, the charge, and discharge currents are assumed to be low enough so that the charge capacity Q_0 change (Peukert effects) is nihil. The charging, or coulombic efficiency due to irreversible parasitic reactions in the battery has been taken into account by using an estimate of the average coulomb efficiency $\bar{\eta}_c = 90.5\%$. Self-discharge, or parasitic current is not separately considered, but these losses are assumed to be modeled by $\bar{\eta}_c$. The SoC is calculated with,

$$SoC(t) = Q(t)/Q_0, \text{ with } \dot{Q}(t) = \bar{\eta}_c \cdot I(t). \quad (9)$$

In Fig. 6(a), R_i as a function of the SoC for charging, and discharging for the spiral wound Ni-MH battery module used in the Prius is shown. In Fig. 6(b), V_{oc} as a function of the SoC is shown[2]. The static efficiency maps for charging, and discharging as a function of the SoC are shown in the figures 6(c), and (d). It can be seen that the influence of the SoC within an usual operation window of $0.3 - 0.8$ is very small. The battery power is well approximated by

$$P_{bat} = \phi_{bat}(SoC|P_s) \approx c_2(SoC|P_s) \cdot P_s^2 +$$
$$\max(c_1^-(SoC|P_s) \cdot P_s, c_1^+(SoC|P_s) \cdot P_s) + c_0(SoC), \quad (10)$$

with $0 < c_1^- < 1$, and $c_1^+ > 1$ for storage devices with losses [12].

C. Transmission efficiency

The power-split CVT for the Prius consists of one planetary gear set, and an electric variator (see Fig. 1(h)). The engine is connected to the carrier, the generator $EM2$ is connected to the sun gear, and the annulus is connected to the output shaft of T, and the motor $EM1$.

1) Loss-free analysis: Generally, for power-split CVTs the speed -, and torque relations in the loss-free case as is shown in [13] can be written as,

$$\left[\begin{array}{c} \omega_{T,i} \\ \omega_{T,o} \end{array} \right] = \left[\begin{array}{cc} a & c \\ b & d \end{array} \right] \cdot \left[\begin{array}{c} \omega_{vi} \\ \omega_{vo} \end{array} \right] = M \cdot \left[\begin{array}{c} \omega_{vi} \\ \omega_{vo} \end{array} \right], \quad (11)$$

$$\left[\begin{array}{c} T_{T,i} \\ T_{T,o} \end{array} \right] = -M^T \cdot \left[\begin{array}{c} T_{vi} \\ T_{vo} \end{array} \right]. \quad (12)$$

The variator -, and transmission speed ratio are respectively defined as,

$$r_v = \frac{\omega_{vo}}{\omega_{vi}} = -\frac{T_{vi}}{T_{vo}} = \frac{(dr + c)}{(br + a)}, \quad (13)$$

$$r = \frac{\omega_o}{\omega_i} = -\frac{T_{T,i}}{T_{T,o}} = -\frac{(ar_v - c)}{(br_v - d)}, \quad (14)$$

resulting from the equilibrium of power at the input, and output shafts of the variator, and the transmission respectively. The variator power ratio Ψ can be written as,

$$\Psi = \frac{P_{vi}}{P_{T,i}} = \frac{r_v}{r} \cdot \frac{dr}{dr_v} = 1 - \frac{z \cdot r_d}{(z-1)} \cdot r, \quad (15)$$

with the matrix elements: $a = 1 - z$, $b = z \cdot r_d$, $c = 0$, $d = r_d$. The variables z and r_d represent the planetary gear -, and final drive ratio.

2) Simplified loss model: At a certain r_{gn}, the ω_{EM2} changes sign causing a mode switch between generator, and motor function, because to much torque is transmitted over the annulus to the vehicle wheels. Then, the $EM1$ switches between motor, and generator function. In addition, with Eq. (13), and with Eq. (15) it can be seen that r_v, and Ψ at $r = r_{gn}$ become,

$$\lim_{r \downarrow \uparrow r_{gn}} r_v = \pm\infty, \ \Psi(r_{gn}) = 0.$$

Then all input power flows over the mechanical branch to the vehicle wheels. The η_T is maximum. Using Eq. (15) r_{gn} becomes,

$$r_{gn} = \frac{(z-1)}{z \cdot r_d}. \tag{16}$$

If $r > r_{gn}$, then $r_v < 0$ causing that also $\Psi < 0$. The η_T is reduced due to negative power circulation. The η_T during positive $P_{vi} > 0$, and negative power flow $P_{vi} < 0$ through the variator becomes,

$$\eta_T = \begin{cases} (\eta_{ps}(1-\Psi) + \eta_v \cdot \Psi) \cdot \eta_{fd}, & P_{vi} > 0, \\ (\eta_{ps}(1+\eta_v \cdot \Psi) - \Psi) \cdot \eta_{fd}, & P_{vi} < 0, \end{cases} \tag{17}$$

with the variables η_{ps}, η_v and η_{fd} representing the efficiency of the planetary gear set, the electric variator, and the final drive with differential. Note that in case of $\Psi < 0$, the absolute value for Ψ has to be used in Eq. (17).

V. DRIVETRAIN CONTROL STRATEGIES

The operation points in the static-efficiency map of an engine, which maximizes the system efficiency are collected by the System Optimal Operation Line (SOOL) for a given engine power level $P_{P,o}$. The optimal engine torque $T_{P,o}^*$, and speed $\omega_{P,o}^*$ for a certain $P_{P,o}$ is pre-scribed in the following research steps by the

1) EOOL incorporating η_P alone;
2) SOOL incorporating all efficiencies.

The EOOL, and the SOOL are numerically pre-computed for all admissible P_s, SoC, $T_{V,i}$, and ω_{Vi} combinations, with using the operation points pre-scribed by the lines as are shown in the Fig. 3, and are stored in a look-up tables. Then, using $T_{P,o}^*$, and $\omega_{P,o}^*$ pre-scribed by the EOOL, or the SOOL, the optimal P_s is calculated by using DP given the drive cycle, and the vehicle parameters.

A. The Energy Management Optimization Problem

The optimization problem is finding the optimal control power flow $P_s(t)$ given a certain power demand at the wheels P_v, while the cumulative fuel consumption M_f is minimized subjected to several constraints, i.e.,

$$J(E_s, P_s) = \min_{P_s} \int_0^{t_f} \dot{m}_f(E_s, P_s) dt, \tag{18}$$
$$\text{s. t. } \vec{h} = 0, \vec{g} \leq 0.$$

where $\dot{m}_f$ is the fuel rate in $[g/s]$. The main constraints are energy conservation balance of E_s over the drive cycle, constraints on the power P_s, and the energy E_s.

$$h_1 := \triangle E_s(t_f) = E_s(t_f) - E_s(0) = 0, \tag{19}$$
$$g_{1,2} := P_{s,min} \leq P_s(t) \leq P_{s,max}, \tag{20}$$
$$g_{3,4} := E_{s,min} \leq E_s(t) \leq E_{s,max}, \tag{21}$$

with the relative energy change $\triangle E_s(t_f)$. Using DP the finite horizon optimization problem is translated into a finite computation problem. Note that in principle the technique results in an optimal solution for the EMS, but that the grid step size also influences the accuracy of the result.

B. Simulation approach

The η_T is determined by $T_{P,o}$, and $\omega_{P,o}$. However, the required $T_{P,o}$, and $\omega_{P,o}$ are determined by η_T, and the required P_v. Due to this causality conflict it is impossible to determine the $T_{P,o}^*$, and $\omega_{P,o}^*$ (pre-scribed by the EOOL, or the SOOL) exactly. In this study the losses in T, and S are estimated, and are compensated in the following procedure:

1) Given the requested P_v, $T_{P,o}^*$, $\omega_{P,o}^*$ are determined without any drivetrain losses at t = 0. Using these values the modified η_T can be calculated;
2) The difference between $P_{P,o}^*$ times the modified η_T, and P_v is used to calculate the modified $P_{P,o}$ at the initial iteration step;
3) The modified $P_{P,o}$ is used to calculate the modified $T_{P,o}^*$, and $\omega_{P,o}^*$ using the EOOL, or the SOOL. The modified η_T is calculated by using the modified $T_{P,o}^*$, and $\omega_{P,o}^*$ at the next iteration step;
4) Steps 2 and 3 are repeated until the power difference between the iteration steps at a certain time step becomes very small;
5) At later time steps the required $P_{P,o}$ can be calculated using the known values for the efficiencies at the previous step. Thereto, the requested P_v is divided by the computed η_T.

VI. SIMULATION RESULTS

A. Model

The vehicle parameters are summarized in the table II. The Japanese drive cycle JP10-15, which is used for comparison, requires the engine to be warmed-up before the test cycle is run. Furthermore, for simplicity, the inertias of the motor, generator, and engine are assumed to be zero. Also, the auxiliary loads are neglected.

TABLE II
RELEVANT VEHICLE PARAMETERS

Parameter	Value	Unit
Mass	1368	$[kg]$
Air drag coefficient	0.29	$[-]$
Frontal area	1.746	$[m^2]$
Roll resistance coefficient	0.9	$[\%]$
Max. Reg. brake fraction	0.5	$[-]$

B. Results, and Conclusions

In Table III the fuel economy results are shown. Note that the measured fuel economy on the JP10-15 of the Toyota Prius (1998) is $3.48 \ [L/100km]$. For comparing the fuel economy results of ADVISOR the "Zero-Delta SoC correction" routine was used, which adjusts the initial SoC until the simulation run yields a zero change in a SoC +/- 0.5% tolerance band.

1) Test 1, and 2: The DP results show that the difference between EOOL, and SOOL for the JP10-15 is small. Analyzing the results from DP, it was found, that the vehicle is propelled up to a certain vehicle drive power P_v only by the motor $EM1$. During braking energy is partially recuperated

up to the maximum generative power limitation of $EM1$, and some of the energy is dissipated in the wheel brake discs. During these modes, also defined as the Motor only (M), and Brake Energy Recuperation (BER) modes, the engine is off, and has no idle -, or drag losses. Additional charging, and discharging during propulsion, when the engine status is on, defined as the Charging (CH) -, and the Motor-Assist (MA) mode, is performed in order to further improve the overall efficiency. Furthermore, the optimal EMS is focussed on charging during driving mainly with $EM2$ in the low speed areas ($< 41 \ [km/h]$), and mainly with $EM1$ in the high speed areas. In the Fig. 7(a), and (b) the relative energy $\triangle E_s$ over time, and the energy distribution between different hybrid modes for the different strategies are shown.

2) Test 3, and 4: Within the implemented sub-optimal strategy of ADVISOR, it was found, that the control parameters: (i) 'the vehicle speed threshold' $v_{min} = 12.5 \ [m/s]$ below which the vehicle is only propelled by the motor $EM1$, and (ii) 'the engine power threshold' $P_{P,min} = 6 \ [kW]$ below the engine is allowed to shut-off mainly determine the EMS, and the fuel economy. Using the results from DP, it showed that the optimal control parameters are $v_{min}^* = 20 \ [m/s]$, and $P_{P,min}^* = 4.5 \ [kW]$. Test 3 showed, that in the high speed areas the engine was not allowed to shut off at relative low P_v, because $v > v_{min}$ resulting in less idle stop, and less generative torque of $EM1$ during braking due to additional engine drag torque. Due to $v_{min}^* > v_{min}$ effectively more (free) energy is charged during the BER mode than during the CH mode which reduces the fuel cost. Although, $P_{P,min}^* < P_{P,min}$ causes that the vehicle is less propelled by $EM1$ during the M mode, which reduces the fuel saving with idle stop, the fuel economy is significantly improved. However, there is still a small difference between DP, and ADVISOR, caused by optimal charging, and discharging during driving. Note that in ADVISOR the engine is also operated at the EOOL.

3) Test 1, 4, and 5: The fuel economy difference between the RB EMS [11], and DP is small. The average constant values for the coefficients c_i of the power based functions describing the characteristics of the components calculated with the results of test 1 are used in test 5. However, the fuel economy of test 5 is better compared to test 4, because the engine is assisted by the motor $EM1$ at some drive power demands resulting in additional fuel savings.

The fuel economy, and the EMS with using a few characteristic parameters describing the component efficiencies, can be calculated very quickly, and with sufficient accuracy. In future work the influence of the topology choice on the fuel economy, and EMS will be investigated.
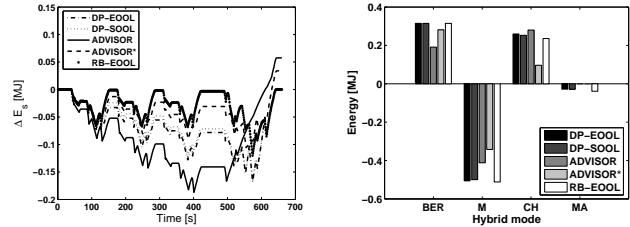
ACKNOWLEDGMENT

TABLE III

FUEL ECONOMY RESULTS

Test	Strategy	Fuel economy [$L/100km$]		
		City	Highway	Combined
1.	DP/EOOL	2.54	3.13	2.84
2.	DP/SOOL	2.56	3.10	2.84
3.	ADVISOR	2.33	4.27	3.34
4.	ADVISOR*	2.82	3.12	2.98
5.	RB/EOOL	2.83	2.97	2.90

*Optimized strategy by changing the control parameters.

(a) Relative energy $\triangle E_s$ over time (b) Energy distribution between the hybrid modes

Fig. 7.   Energy distribution between different hybrid modes, and relative energy over time for the different strategies.

REFERENCES

[1] Powell, B. K., Bailey, K. E., and Cikanek, , S. R., *Dynamic Modeling and Control of Hybrid Electric Vehicle Powertrain Systems*,   In: J. of IEEE-Control Syst. Mag., **18**(5), p.17–33, 1998.

[2] Wipke, K. B., Cuddy, M. R., and Burch S. D., *ADVISOR 2.1: A User-Friendly Advanced Powertrain Simulation Using a Combined Backward/Forward Approach*,   In: J. of IEEE-Trans. on Vehicular Technology, **48**, p.1751–1761, 1999.

[3] Butler, K. L., Ehsani, M., and Kamath, P., *A Matlab-Based Modeling and Simulation Package for Electric and Hybrid Electric Vehicle Design*,   In: J. of IEEE-Trans. on Vehicular Technology, **48**, p.1770–1778, 1999.

[4] G. Rizzoni, L. Guzzella, and B. M. Baumann, *Unified Modeling of Hybrid Electric Vehicle Drivetrains*,   In: J. of Transactions on Mechatronics, **4**(3), p.246–257, 1999.

[5] L. Guzzella, and A. Amstutz, *CAE Tools for Quasi-Static Modeling and Optimization of Hybrid Powertrains*,   In: J. of Transactions on Vehicular Technology, **48**(6), p.1762–1769, 1999.

[6] H.M. Kim, M. Kokkolaras, L.S. Louca, G.J. Delagrammatikas, N.F. Michelena, Z.S. Filipi, P.Y. Papalambros, J.L. Stein, and D.N. Assanis, *Target cascading in vehicle redesign: a class VI truck study*,   In: J. of Vehicle Design, **29**(3), p.199–225, 2002.

[7] A. Sciaretta, L. Guzzella, and C.H. Onder, *On the power split control of parallel hybrid vehicles: from Global Optimization towards Real-time Control*,   In: J. of Automatisierungstechnik, **51**(5), p.195–205, 2003.

[8] M. Koot, J.T.B.A. Kessels, B. de Jager, W.P.M.H. Heemels, P.P.J. van den Bosch, and M. Steinbuch, *Energy management strategies for vehicular electric power systems*,   In: J. of IEEE-Trans. on Vehicular Technology, **54**(3), p.771–782, 2005.

[9] K.J. Kelly, M. Mihalic, and M. Zolot, *Battery usage and thermal performance of the Toyota Prius and Honda Insight for various chassis dynamometer test procedures*,   In: NREL/CP-540-31306, p.1–6, 2001.

[10] K.J. Kelly, and A. Rajagoplan, *Benchmarking of OEM Hybrid Electric Vehicles at NREL*,   In: NREL/TP-540-31386, p.1–101, 2001.

[11] T. Hofman, M. Steinbuch, A. Serrarens, and R. van Druten, *Rule-based energy management strategies for hybrid vehicle drivetrains: A fundamental approach in reducing computation time*,   In: Proc. of 4th IFAC-Symposium on Mechatronic Systems, Heidelberg, Germany, 2006.

[12] B. De Jager, *Predictive storage control for a class of power conversion systems*,   In: Proc. of the Europ. Control Conf., Cambridge, UK, 2003.

[13] J. W. Polder, *A network theory for variable epicyclic gear trains*,   Ph.D. Thesis, Technische Universiteit Eindhoven, 1969.